View metadata, citation and similar papers at core.ac.uk

brought to you by CORE

provided by NASA Technical Reports Server

N71-17879

NASA CR 116443

FINAL TECHNICAL REPORT - PHASE III

RESEARCH ON LOW VOLTAGE ELECTROLUMINESCENT DEVICES WITH STORAGE

J.M. HANLET
&
H. SHIMIZU

JUNE 1970

CONTRACT NO. NAS 12-545

CASE FILE COPY

Prepared By:
THE MARQUARDT COMPANY
CCI Aerospace Corporation
16555 Saticoy Street
Van Nuys, California

For:
NATIONAL AERONAUTICS AND SPACE ADMINISTRATION
Electronics Research Center
Cambridge, Massachusetts

Mr. Edwin Hilborn
Technical Monitor
NAS 12-545
Electronics Research Center
575 Technology Square
Cambridge, Massachusetts 02139

Requests for copies of this report should be referred to:

NASA Scientific and Technical Information Facility
P. O. Box 33, College Park, Maryland 20740

This report covers the third phase of above mentioned NASA Contract. The first and second phases of this research have been respectively reported in NASA CR 86060 and NASA CR 86344.

Mr. J. Hanlet - Principal Investigator

THE MARQUARDT COMPANY REPORT NO. RPT 102

THE Marquardt CORPORATION VAN NUYS, CALIFORNIA

RESEARCH ON LOW VOLTAGE ELECTROLUMINESCENT DEVICES WITH STORAGE

Jacques M. Hanlet
&
H. Shimizu

June 1970

Prepared under Contract No. NAS 12-545 by

THE MARQUARDT COMPANY
CCI Aerospace Corporation
Van Nuys, California

For:

NATIONAL AERONAUTICS AND SPACE ADMINISTRATION
Electronics Research Center
Cambridge, Massachusetts

TABLE OF CONTENTS

Summary	1
Introduction	2
Heterojunction Theory	3
The ZnSe-AlAs System	3
The Schottky Junction	11
Experimental	15
Preparation of AlAs	15
Preparation of ZnSe-AlAs Junction	15
Preparation of Pt-ZnSe Junction	20
Demonstration Models	21
Conclusions and Recommendations	22
References	23
Appendix I	
Vaporization of AlAs	24
Appendix II	
Optical Method for Band Gap Determination	28
Appendix III	
Electroluminescent Model	31
Appendix IV	
New Technology	41

SUMMARY

A study has been directed toward the development of efficient electroluminescent systems operable at room temperature and applicable to storable and erasable visual read out devices. As the result of a continuing study, this phase of work included the preparation and characterizations of the heterojunction ZnSe-AlAs and the Schottky junction Pt-ZnSe.

Polycrystalline AlAs was prepared by reaction of arsenic vapor with molten aluminum. Polycrystalline AlAs constituted the source for epitaxial deposition on crystalline ZnSe substrate. Thermodynamic considerations indicated that the direct evaporation of AlAs was feasible. AlAs was deposited on the natural (110) face of a ZnSe single crystal using a Knudsen type effusion system for AlAs evaporation. Initial results were not conclusive in that the film was not sufficiently adherent to the substrate to perform electronic characterizations. The substrate had also undergone deterioration of luminescent behavior from the cumulative thermal exposure during preliminary parametric studies. Comparative preliminary investigations were made on a Schottky emission junction of platinum evaporated on a single crystal ZnSe surface.

A method was developed for the determination of optical constants in complex thin films by measuring transmittance from interference patterns. This provides a method for junction band gap calibrations directly on the films in place of the usual magneto-resistance method which requires a relatively large, self-supporting specimen.

The performance of a demonstration multielement model consisting of sections of a large area thin film Pt-ZnSe p-i-n junction is described. The thin film ZnSe was deposited on the basal plane surface of a sapphire crystal plate onto which a pattern of platinum was deposited.

Although sufficient experimental results were not obtained, the analytical investigations indicate that these systems hold promise of improved electroluminescent properties.

INTRODUCTION

The prospects of a solid state electroluminescent (EL) device of high brightness and efficiency without heat generation has lead to an increased level of activity among workers in the semiconductor field. The underlying basis for electroluminescence is the injection of carriers, either electrons or holes, under a potential field, into a region containing their conjugate so that electron-hole recombinations can occur with the release of energy in the visible spectral region. This report describes the third phase of a continuing program to develop a bright EL system which is operable at room temperature and to demonstrate its applicability to a multi-element, two dimensional array which can provide storable and erasable pictorial representations.

During Phase I,[(1)*] a survey of various II-VI, III-V and IV-IV compounds was made finally listing prospective EL materials with wide band gap and good stability in air. From this list, the ZnTe-ZnSe system was selected for initial thin film investigations. During this phase, the concept of storage and erasability was demonstrated by a breadboard model of multiple EL and avalanche diode sets. Phase II[(2)] efforts included the continuation of ZnTe-ZnSe investigations and the beginning of new studies of the ZnSe-Pt heterojunction system. During this work, a major contribution to thin film technology was the development of a deposition system with concentric dual vaporization sources with independent temperature controls. A thermal ionization accessory was incorporated to thermally dissociate dimeric chalcogen vapors to the monomeric form for epitaxial depositions of less defective films.

The purpose of the Phase III effort was to develop an EL heterojunction based on the ZnSe-AlAs or Pt-ZnSe Schottky system to provide improved efficiencies at room temperature. The early studies on this program and the studies to date of electroluminescence by others have shown sufficient brightness only under cryogenic conditions. The ZnSe-AlAs combination holds promise from the standpoint of good compatibility in crystalline structure, lattice parameter and band gap and is thermally stable. An apparent incompatibility arises from the nature of the transitions, the ZnSe transition being direct and the AlAs transition being indirect. One of the purposes of this study was to determine the consequence of this difference.

*References at end of report

HETEROJUNCTION THEORY

The ZnSe-AlAs System

ZnSe and AlAs are isotypic, both having the FCC, zincblende structure with almost identical lattice dimensions as shown in Table I, which lists selected properties for the two compounds. ZnSe also crystallizes in a metastable hexagonal wurtzite-type structure with cell dimensions of $a \cong a_c / \sqrt{2}$ and $c \cong 2a_c / \sqrt{3}$ where a_c is the cubic lattice parameter. For the heterojunction, however, only the cubic form is of importance. In addition to structural compatibility, ZnSe and AlAs have other properties in common as can be noted in the table. Further, ZnSe and AlAs are the only compounds which form in their respective phase systems. Both are quite stable as indicated by the relatively high melting points. The respective congruent melting points occur at pressures above l atmosphere. In the zincblende structure (as well as in wurtzite) all atomic bonding are tetrahedral and essentially covalent. The covalent radii of some of the Groups II, III, V, VI atoms are shown in Table II. Within the accuracy of the significant figures listed, the interatomic spacings for Zn-Se and Al-As, as expressed by the sum of the radii, are equal. For zinc blende, the closest interatomic distance is related to the lattice parameter by $d = \frac{a\sqrt{3}}{4}$. The closest Zn-Se distance (a = 5.6686 A) is 2.455 A while for AlAs (a = 5.66Z A) it is 2.451 A compared to the estimated distances from the table of 2.45 A and 2.44 A, respectively.

The replacement of a Zn atom in ZnSe with a Group III donor metal (Al, Ga, In) results in a n-type material provided Zn vacancies are not formed. Such vacancies act as self-compensating acceptors. Since there is a tendency for these vacancies to form during doping, it is necessary to provide an over-pressure of Zn to prevent the loss of zinc from the crystal lattice during high temperature processing.

Very little information is available on AlAs, but there has been a recent upsurge of activity in the study of the material.[3,4] Although there has been indications to the contrary, some work on this program on the synthesis of AlAs and some of the recent information just cited, show that AlAs is quite stable in air if the material is well crystallized.

The effectiveness of the heterojunction depends on many factors all of which must be favorable.

1. Both the n-ZnSe and p-AlAs must be reasonably conductive to avoid excessive ohmic losses.

TABLE I

PROPERTIES OF AlAs AND ZnSe

	AlAs	Ref.	ZnSe	Ref.
Melting Point	1773°C @1.7 atm.	3	1515 ± 20°C	7
Structure	FCC (Zincblende) a = 5.655 ± 0.002	6	FCC (Zincblende) a = 5.667	8
Lattice Parameter (R.T.)	a = 5.662 Å	3	a = 5.6686 ± 0.0006Å	9
Band Gap	2.16 (Indirect) 2.9 (Direct)	4 5	2.6 (direct)	
Thermal Coef. of Expansion (per °C)	5.20×10^{-6} (20-1000°C)	4	9.44×10^{-6} (20-520°C)	10
Conduction Type	amphoteric;normally n-type p-(with Zn Dopant)	3	n-type	
Heat of Formation (298°K)	35.4 kcal/mole	6	39 kcal/mole	11
Index of Refraction	3.094	3	2.89	12

TABLE II

ELEMENTS PROPERTIES

Element	Group	Structure	Covalent Radius Å *	Electro-negativity**
Zn	IIB	(Ar) $3d^{10}$ $4s^{2}$	1.31	1.66
Al	IIIA	(Ne) $3s^{2}$ $3p^{1}$	1.26	1.47
Ga	IIIA	(Ar) $3d^{10}$ $4s^{2}$ $4p^{1}$	1.26	1.82
In	IIIA	(Kr) $4d^{10}$ $5s^{2}$ $5p^{1}$	1.44	1.49
P	VA	(Ne) $3s^{2}$ $3p^{3}$	1.10	2.06
As	VA	(Ar) $3d^{10}$ $4s^{2}$ $4p^{3}$	1.18	2.20
Se	VIA	(Ar) $3d^{10}$ $4s^{2}$ $4p^{4}$	1.14	2.48

* L. Pauling, The Nature of the Chemical Bond, Cornell University Press, N.Y., 1960, 3rd ed.

** A. L. Allred, E. G. Rochow - J. Inorg. Nucl. Chem. 5-264 -(1958)

2. Both elements as well as the junction must be relatively free of defects to minimize non-radiative recombinations. The close matching of lattice parameter and continuity of structure through the junction is therefore, imperative.

3. The system must be energetically compatible, i.e., both materials must have similar band gaps which are sufficiently wide to produce E. L. emission in the visible region whether the radiative recombination occurs by electron and/or hole injection across the interface.

Even if these conditions are satisfied, there are other requisites associated with the fabrication of the junction. Thus, not only is there a need for matching of the lattice parameter at the use temperature, but also a reasonable match through the entire thermal processing cycle so that no destructive strain results from mismatched thermal expansion characteristics.

Fabrication techniques which result in continuity of the atomic lattice and band structure should minimize imperfections which would be centers for nonradiative recombinations. If good lattice and band structure matching is effected, the mechanism of electroluminescence may be difficult to distinguish from that of a quasi-homojunction especially if there is a small region of solid solution and the respective cation and anion sublattices are in registry at the interface. Figure 1 shows the energy vs. k-space diagrams for ZnSe and AlAs together with a hypothetical energy-composition diagram. Number II-VI compounds do not form complete solid solutions with III-V compounds but may show limited degrees of intersolubility. The minimum band gap for ZnSe, a direct transition, is approximately 2.6 eV. Although AlAs has a direct transition band gap of 2.9 V, the existence of a lower energy indirect band gap of 2.16 eV makes the probability of the direct transition very low. The indirect transition energy in ZnSe is sufficiently higher than the direct transition energy that it is inconsequential. Any solubility of ZnSe in AlAs, however, would raise the indirect transition energy of AlAs. If a complete solid solution were to exist,there would be a crossover composition at which the direct and indirect band gaps were equal, the value of which would be greater than 2.6eV. Although there is no extensive solid solution, a well-matched interface and interdiffusion of a few atomic layers may constitute an equivalent solid solution.

In an injection electroluminescent diode, the carrier is generally injected from the higher to the lower band gap material. Thus in Figure 2a, a schematic representation of the band structure of the heterojunction, electrons are shown to be injected from ZnSe into AlAs, resulting in an indirect recombination with emission of light of energy somewhat less than 2.16 eV depending on the depth of the acceptor level in AlAs. The time delay associated with the momentum mismatch in the indirect

BAND GAPS IN ZnSe AND AlSe AND A HYPOTHETICAL Eg-COMPOSITION DIAGRAM FOR ZnSe-AlAs

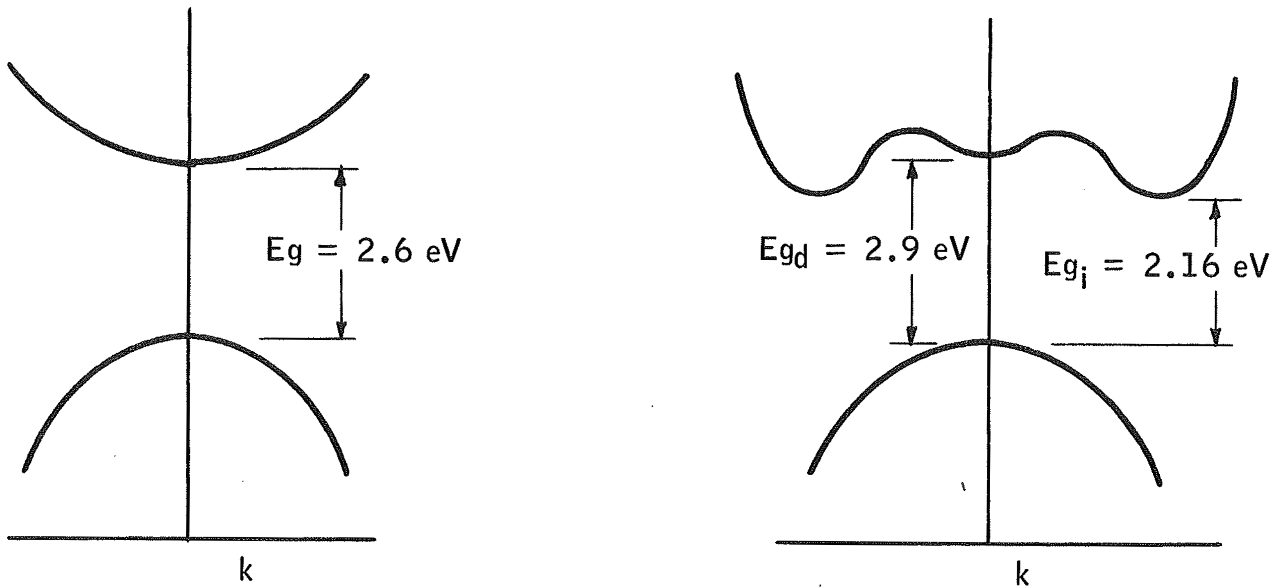

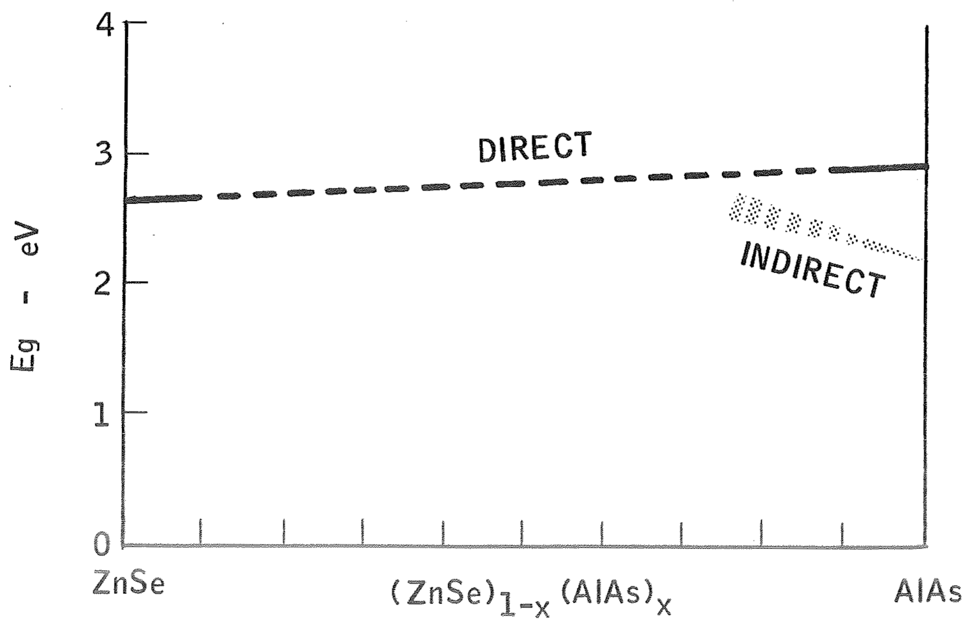

Figure 1

BAND MODEL FOR ZnSe - AlAs JUNCTIONS

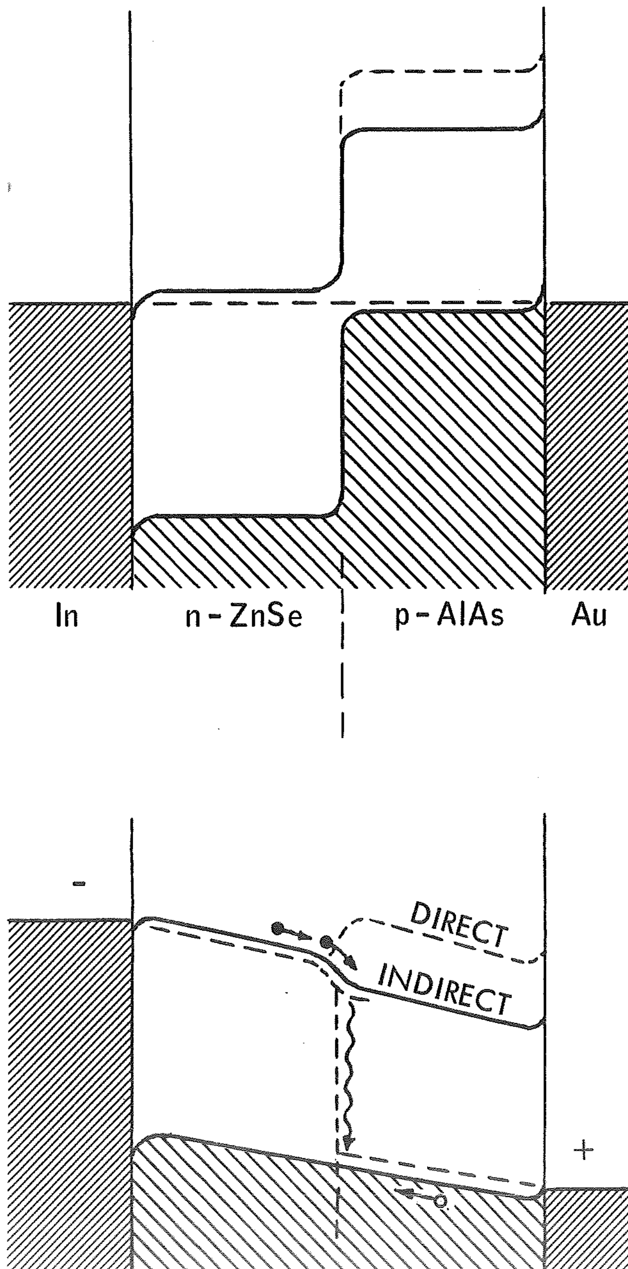

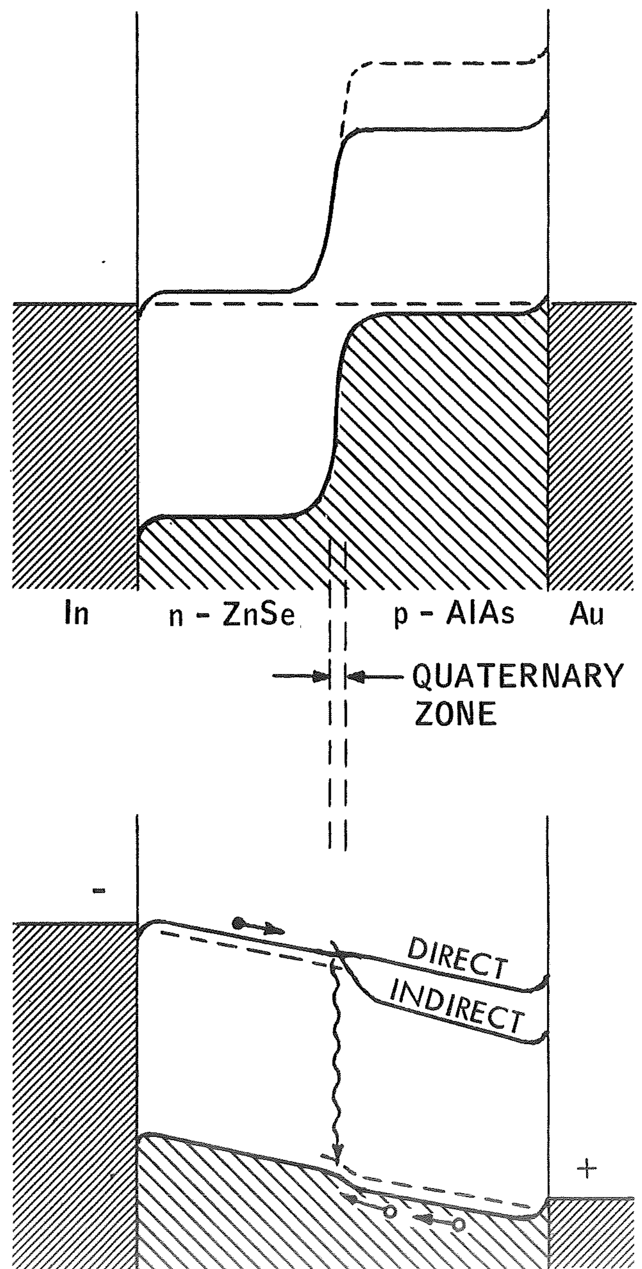

transition may allow nonradiative recombinations to occur, thus reducing efficiency for electroluminescence. The possibility of the formation of a quaternary solid solution at the interface, however, may permit direct transitions to occur by hole injection from this zone into the n-ZnSe. For this transition, the radiated energy would be 2.6 eV less the depth of the acceptor level as represented in Figure 2b.

Looking at the heterojunction more analytically, for the isolated semiconductors, the energy band profile at equilibrium is shown in Figure 3a. When the junction is made, the Fermi levels coincide on both sides and the vacuum level is continuous and parallel to the band edges, Figure 3b. The discontinuity in conduction ΔEc, ΔEv, is invariant with doping, i.e., Eg and EA are not function of doping with non-degenerate semiconductors. *The internal potential V_b is the sum of V_{b1} and V_{b2}, i.e., of the* electrostatic potentials supported by the respective semiconductors constituting the junction. The width of the depletion layer is obtained by solving Poisson's equation (discussed in Appendix III) with the boundary condition:
$\epsilon_1 E_1 = \epsilon_2 E_2$ at the interface, we have,

$$d_1 = \left[\frac{2N_{a2}\ 1\ 2\ (V_{b1} - V)}{eN_{d1}\ (\epsilon_1 N_{d1} + \epsilon_2 Na_2)} \right]^{\frac{1}{2}}$$

$$d_2 = \left[\frac{2N_{d1}\ \epsilon_1\ \epsilon_2\ (V_{b1} - V)}{eN_{a2}\ (\epsilon_1 N_{d1} + \epsilon_2 N_{a2})} \right]^{\frac{1}{2}}$$

The junction capacitance is then,

$$C = \left[\frac{e\ N_{d1}\ N_{a2}\ \epsilon_1\ \epsilon_2}{2\ (\epsilon_1\ N_{d1} + \epsilon_2\ N_{a2})\ (V_{b1} - V)} \right]^{\frac{1}{2}}$$

and the relative voltage supported by each semiconductor comprising the heterojunction is

$$\frac{V_{b1} - V_1}{V_{b2} - V_2} = \frac{N_{a2}\ \epsilon_2}{N_{d1}\ \epsilon_1}$$

with $V = V_1 + V_2$

HETEROJUNCTION BAND MODEL

(a) ENERGY RELATION BETWEEN ISOLATED SEMICONDUCTORS

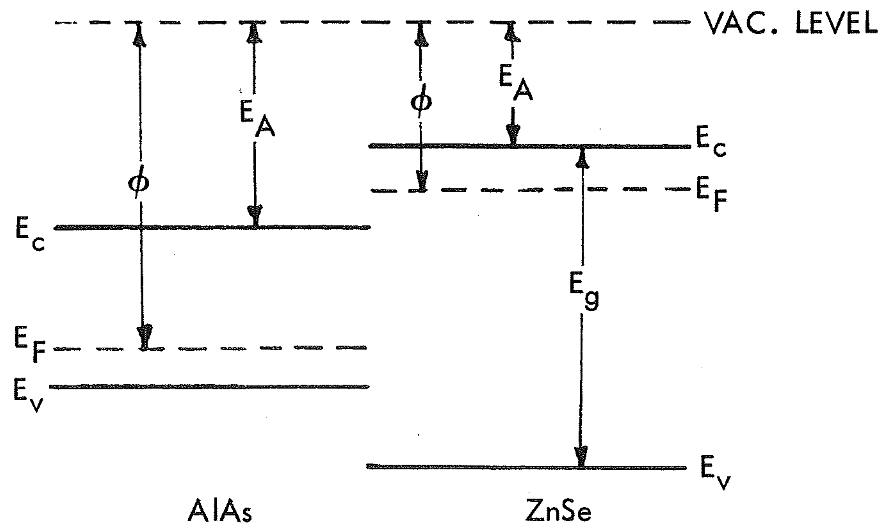

(b) ENERGY RELATION OF AlAs-ZnSe HETEROJUNCTION AT THERMAL EQUILIBRIUM

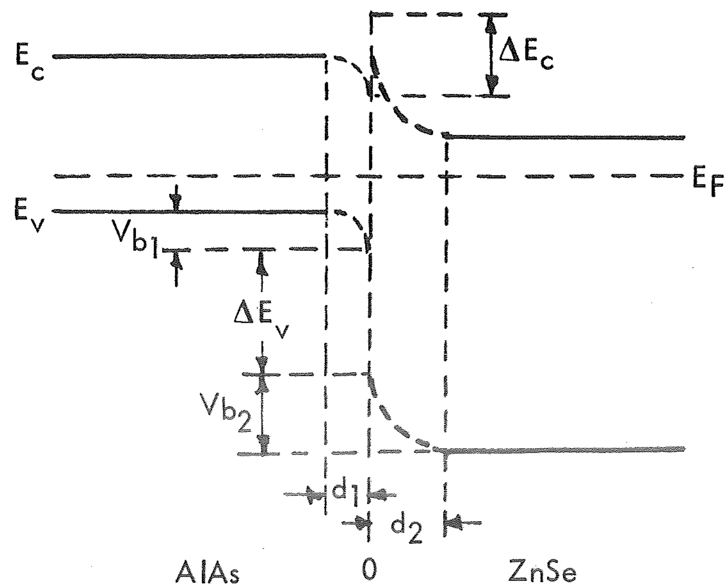

Figure 3

SCHOTTKY JUNCTION

A form of electroluminescent device, which is appealing because of its structural simplicity, was investigated earlier during this work. The junction is based on the combination, metal-semiconductor, with platnium and n-type doped zinc selenide.

The metal-semiconductor system, gives the closest approximation to an abrupt junction whose performance depends mostly on thickness of interfacial and depletion layers. The barrier height ϕ_o, which reduces the outflow of electrons, is defined as a function of the metal work function ϕ_M and the semiconductor electron affinity E_A. The model of such barrier is shown in Figure 4, which is represented by the expression,

$$\phi_o = \varphi_M - E_A \qquad 1.$$

The value of ϕ is mostly determined by the semiconductor surface state density D_s (states $cm^{-2} e.V^{-1}$) whose charge is,

$$Qs = -eD_s \, (Eg - e\,\phi_s - e\,\phi_B - e\Delta\phi) \text{ Coulomb } cm^{-2} \qquad 2.$$

where e is the electron charge, Eg the band gap, ϕs energy level at surface, and $\Delta\phi$ image force barrier lowering which is expressed by,

$$\Delta\phi = \left(\frac{eE}{4\pi\epsilon}\right)^{\frac{1}{2}} = 2\,Ex \qquad 3.$$

The quantity in parenthesis in (2) represents the difference between the Fermi level at the surface and $e\,\phi_s$, while x is the distance between electron subjected to the field and the metal. For $x > w$, where w is the depletion width, w is given by,

$$w = \left[\frac{2\,\epsilon_s}{e\,N_d}\left(V_b - V - \frac{kT}{e}\right)\right]^{\frac{1}{2}} \qquad 4.$$

ELECTROLUMINESCENT SCHOTTKY DIODE

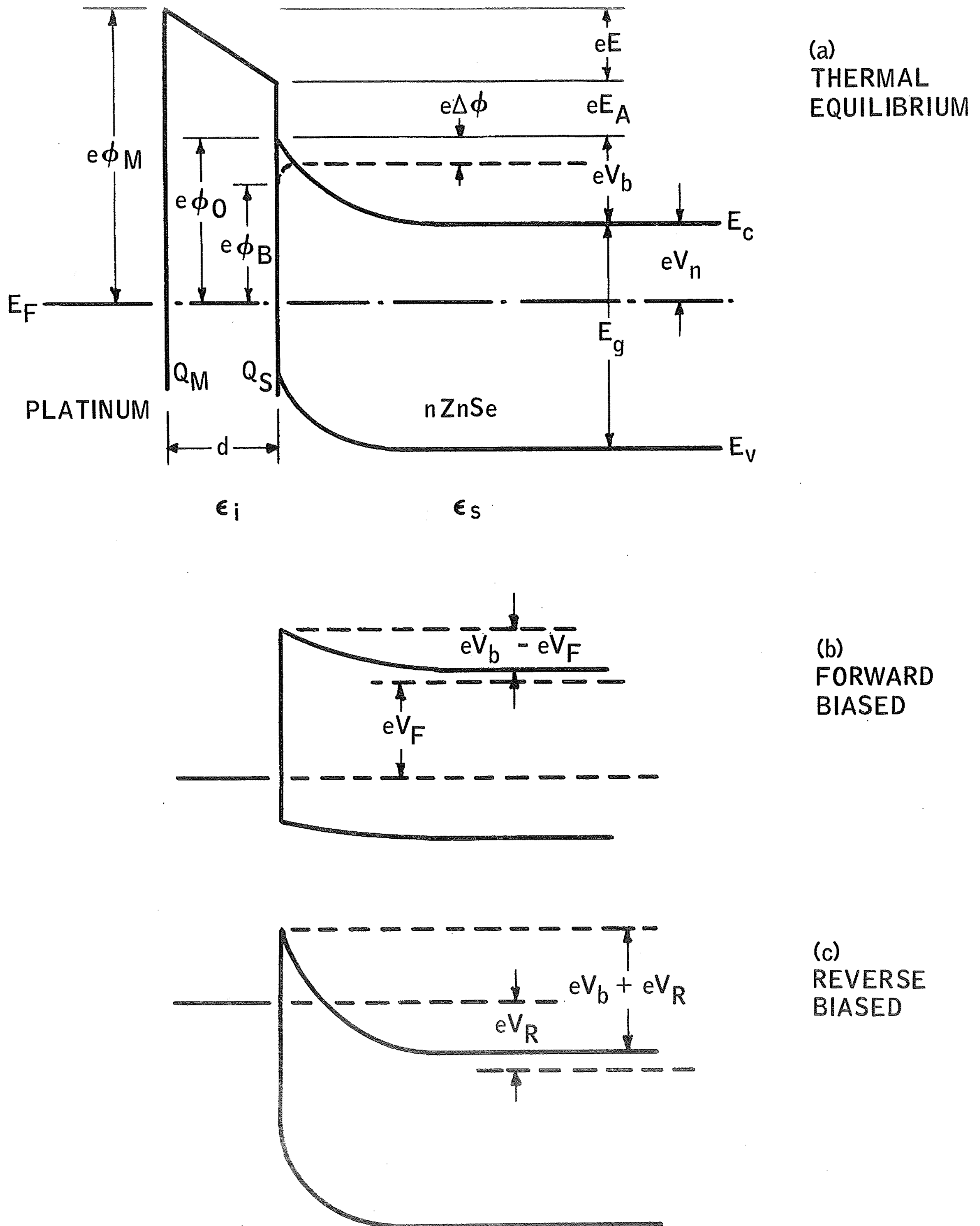

Figure 4

The space charge which forms in this deflection layer n is,

$$Q_{sc} = eN_d \quad w = \left[2e \ \epsilon_s N_d \left(V_b - V - \frac{kT}{e}\right) \right]^{\frac{1}{2}}$$

or

$$Q_{sc} = \left[2e \ \epsilon_s N_d \left(\phi_o - V_n + \Delta\phi - \frac{kT}{e} \right) \right]^{\frac{1}{2}} \text{ Coulomb cm}^{-2} \qquad .5$$

The deflection layer capacitance C per unit area is,

$$C = \left[\frac{e \epsilon_s \ N_d}{2(\phi_o - V - \frac{kT}{e})} \right]^{\frac{1}{2}} = \frac{\epsilon_s}{w} \qquad \text{Farad cm}^{-2} \qquad .6$$

The total charge developed on the metal surface is then,

$$Q_M = -(Q_s + Q_{sc}) \qquad .7$$

and the potential across the interfacial layer metal-semiconductor,

$$E = -d \ \frac{Q_M}{\epsilon_i} \qquad .8$$

where d and ϵ_i are respectively the thickness and permitivity of this interfacial layer. Since from Figure 3

$$E = \phi_M - (E_A + \phi_B + \Delta\phi) \qquad .9$$

which after substitution for Q_M reduces to,

$$\phi_B = \frac{\epsilon_i}{(\epsilon_i + e^2 dDs)} (\phi_M - E_A) + \left(1 - \frac{\epsilon_i}{(\epsilon_i + e^2 dDs)}\right) \left(\frac{Eg}{e} - \phi s\right) - \Delta\phi \qquad 10.$$

Assuming a voltage drop V_o across the space charge region the electron current density $-J_e$ takes the form,

$$-J_e = A \exp \left[-e (\phi_B - V_o) / kT \right] \qquad 11.$$

and for $V_o \simeq 0$ $J_e \approx J_s$ with J_s the saturation current,

$$-J_s \simeq A \exp (-e \, \phi_{B/kT}) \qquad 12.$$

with A the Richardson constant

$$A = N_d \; e(kT/2 \; \pi \, m_e^*)^{\frac{1}{2}} \qquad 13.$$

with m_e^* the effective electron mass.

The total current density is then,

$$J = -J_s - J_e \approx J_s \left[\exp (V_{o/kT} - 1) \right] \qquad 14.$$

The value of N_d may be obtained from the plotting of $1/C^2$ versus voltage

$$N_d \simeq \frac{2}{e \; \epsilon_s} \quad \frac{(-dV)}{d(1/C^2)}$$

EXPERIMENTAL

Preparation of AlAs

Preliminary efforts in the preparation of AlAs were made by passing arsenic vapor over molten aluminum. The As vapor source was maintained at 477°K while the aluminum was maintained at 1283°K, the temperature being regulated to ± 1°K. A cooler zone was maintained at 1223°K in order to condense out any AlAs carried away from the principal mass by the flowing As vapor. A polycrystalline mass was obtained, the color of which ranged from very light orange to a slightly brownish. A sample was taken from both regions and evaluated for structure and lattice parameter by X-ray diffraction. The data from the Dehye-Scherrer pattern shown in Figure 5. are tabulated in Table III. All lines on the film were attributable to AlAs or to unreacted aluminum. The structure was verified to be face-centered cubic with a = 5.6568 A.

The sizes of the crystallites were not adequate for a back reflection Laue pattern nor to obtain coherent optical measurements and information on bond structure. Electrical data obtained from thermal excitation measurements indicated a p-type material with conductivity of 200 mhos and mobility of approximately 16 $cm^2\ volt^{-1}\ sec^{-1}$.

Preparation of ZnSe - AlAs Heterojunction

The availability of ZnSe in single crystal form determined its choice as the substrate and AlAs as the depositant. Several methods are available for the epitaxial growth of AlAs films on oriented substrates.

1. Deposition from direct evaporation of AlAs.
2. Deposition from elemental Al and As.
3. Chemical vapor deposition from AlCl and AsH_3

The first method is the most direct if AlAs is available. This method presumes that the population density of Al and As in the vapor phase are not greatly unequal and that the influence of the heated substrate to cause epitaxial deposition will also tend to confer stoichiometry on the deposit. The second method requires the independent control of the two sources as well as the substrate. With the establishment of suitable parameters, precise stoichiometry is feasible as was shown for ZnSe films produced during Phase II of this program. The third method requires substrate temperature in the range 1200-1250° C.(13) This temperature was considered excessive for ZnSe. Such high temperatures would also magnify the effects of thermal expansion mismatch.

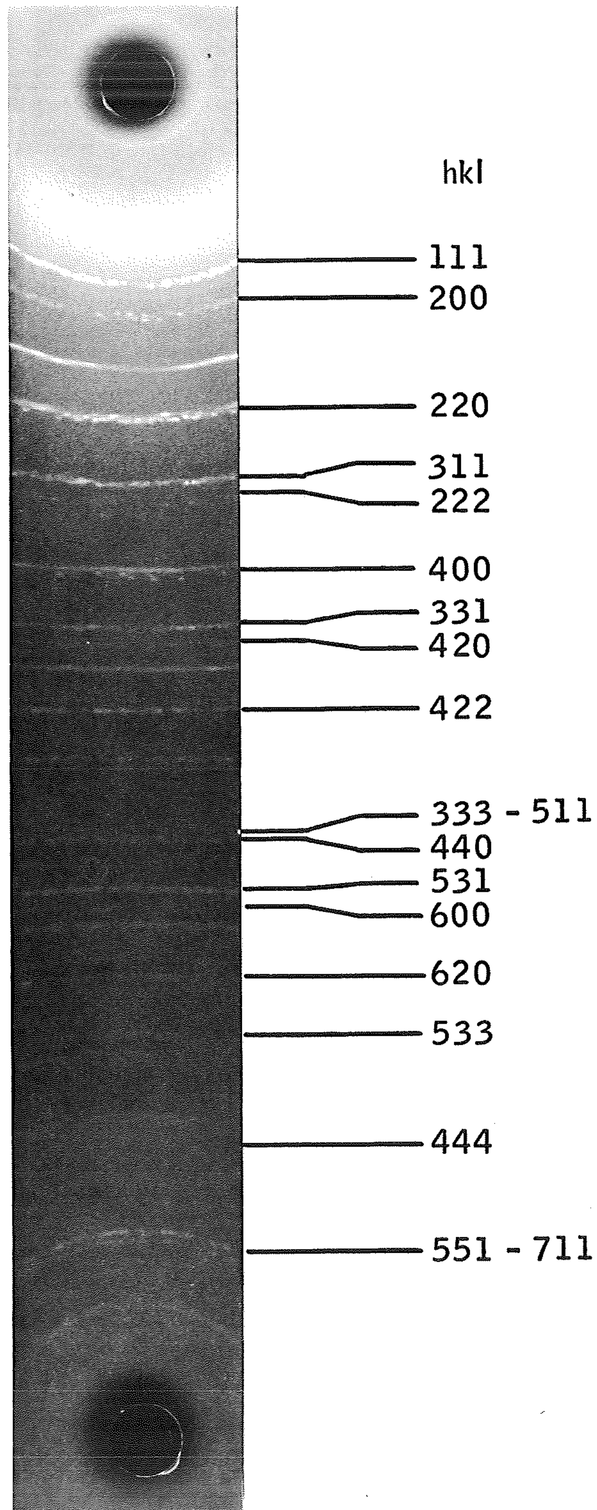

ALUMINUM ARSENIDE DIFFRACTION PATTERN

TABLE III

Lattice Spacing AlAs Marquardt #5424-01

Lines *	d spacing Å	I/I_o	hkℓ	a_o
1	3.26	100	111	5.646483
2	2.83	20	200	5.660000
3	2.00	50	220	5.656860
4	1.705	30	311	5.654837
5	1.633	V.W.	222	5.646483
6	1.413	V.W.	400	5.640000
7	1.30	10	331	5.666570
8	1.265	V.W.	420	5.657257
9	1.155	10	422	5.658321
10	1.09	W.	333	5.663803
11	1.00	5	440	5.656850
12	.957	10	531	5.661688
13	.944	W.	600	5.664
14	.895	W.	620	5.660472
15	.863	W.	533	5.659053
16	.816	V.W.	444	5.653411
17	.7925	5	551	5.659583

a = 5.6568 Å Cubic $F\bar{4}3m$

*All other lines appearing in the pattern are assigned to aluminum.

In order to expedite the preparation of the ZnSe-AlAs junction, ZnSe in the single crystal form and AlAs of 5N purity in polycrystalline form were purchased. The ZnSe crystal was approximately 3 x 4 x 5 mm in irregular dimensions with the 4 x 5 faces being the (110) planes of the FCC structure. The crystal had a number of internal cracks and major holes. The crystal was sliced into three sections approximately 1mm thick with a diamond wire saw. An outer slice which had the better natural surface was selected and the opposite surface was ground and polished with 6μ diamond paste. The specimen was etched in a concentrated sulfuric acid-potassium dichromate solution and the excess selenium left on the surface was washed with a concentrated NaOH solution and finally with distilled water. This etching system is selective for the (110) family of planes of ZnSe. Figure 6 shows a back reflection Laue pattern from the 110 face.

The ZnSe crystal and AlAs were placed in their respective holders in the evaporation vacuum chamber. A small vitreous carbon closed-end tube was found suitable for holding AlAs. A diffusion-ion-sublimation pump system was used and the deposition was conducted at approximately 1 x 10^{7} torr.

The substrate was held at a temperature of 425°C and the AlAs source was heated to about 1080°C while the remainder of the quartz cell was maintained at about 600°C. When the system reached equilibrium a shutter screening the specimen was opened to expose substrate specimen to the Al+As effusion stream for 60 minutes. A quartz oscillating crystal placed adjacent to the substrate crystal to monitor the deposition rate did not function properly during this run. Since no other provision was made to determine the deposition rate or the final film thickness, the thickness of the epitaxial deposit could not be ascertained.

The deposit was a transparent amber-red color. The adherence was quite poor in that any unintentional abraision easily scratched and removed the film in the abraided region. For a quick assessment of the luminescent characteristics, the crystal and film was observed under ultraviolet radiation. No fluorescent activity could be detected at room temperature. The crystal was immersed in liquid nitrogen but still showed no UV fluorescent activity in the film or in the interface. The cryogenic treatment proved destructive to the film; the film was lost, probably by thermal shock.

The ZnSe substrate crystal which previously showed activity in the green spectral region at liquid-N_2 temperatures, now showed weak red activity. It is presumed that during the preliminary equipment check out and during the final deposition run, in which the substrate crystal was subjected to an accumulated exposure of about three hours to temperatures in the 400-450°C range at high vacuum, the crystal suffered a selective loss of Se to form deep recombination centers, thus lowering the emitted energy.

BACK REFLECTION LAUE PATTERN FOR ZnSe (110) PLANE

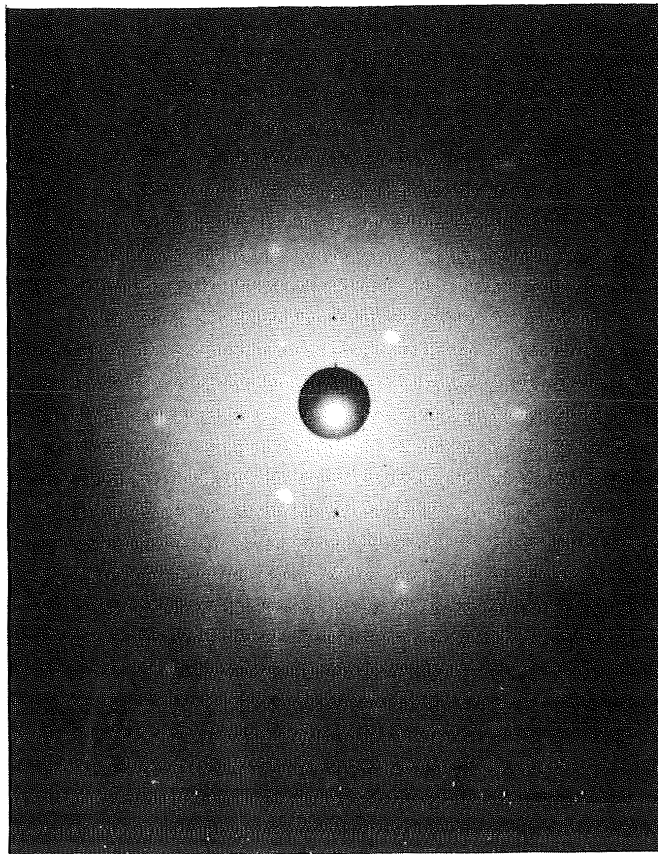

Preparation of Pt-ZnSe Schottky Junction

An alternate electroluminescent junction based on the injection of electrons into an n-type semiconductor (ZnSe) from a high work function metal (Pt) was prepared by high vacuum evaporation. An all metal Varian vacuum system was evacuated to 10^{-9} torr by an ion pump and titanium sublimation pump system after pre-evacuation with an air pump and cryogenic absorption pump system. Platinum was deposited on an original (110) face of a ZnSe crystal. The crystal had been etched in a H_2SO_4 - $K_2Cr_2O_7$ solution, cleaned in NaOH to remove surface Se, and rinsed in distilled water and methanol.

Prior to deposition of the platinum, the ZnSe substrate was degassed in vacuum by thermal cleaning of the surface and by ionic bombardment. In both cases the energy involved was maintained well below the enthalpy for the production of selenium vacancies. The object was clearly to secure a minimum thickness of the residual barrier in order to obtain a greater transparency to electrons and a minimum band bending.

Since the vapor pressure of Pt is low at its melting point, the deposition was performed in several steps to prevent undue elevation of temperature of the ZnSe substrate. The total thickness of Pt deposited on the ZnSe crystal was such as to confer the metal bulk properties to the film.

DEMONSTRATION MODELS

Two models of multi-element electroluminescent device were planned for this program. The first model utilized the ZnSe deposition technology developed in Phase II of this program. The model consisting of seven elements selected from a 4 x 5 array was constructed and delivered at the end of Phase II activities. The junctions were formed by depositing ZnSe epitaxially on the basal plane of a sapphire crystal and subsequently depositing a pattern of platinum electrodes on the resulting ZnSe (III) plane. The characteristics of a representative p-i-n junction was described in the Phase II final report (2) and is repeated in this report as Appendix III.

The second model which had been planned for this program depended on the successful preparation of the ZnSe - AlAs heterojunction. Since the preparation and characterization of this junction are still in progress, the model construction has been postponed.

CONCLUSIONS AND RECOMMENDATIONS

Theoretical analyses continue to indicate high promise of improved electroluminescence both in terms of brightness and efficiency for the ZnSe-AlAs and Pt-ZnSe systems. Experimental difficulties have prevented the achievement of the desired properties, but the experience gained in this study point to methods of correcting the problems which were encountered.

Polycrystalline AlAs can easily be prepared by passing gaseous As_2 over molten aluminum. This material can serve as an evaporative source for the epitaxial thin-film deposition of single crystal AlAs on an isotypic substrate of compatible lattice dimensions.

Additional parametric studies on the evaporation and deposition of AlAs are required to define conditions to obtain epitaxial films without damaging the electronic properties of the ZnSe crystal substrate. The thin film technology must be expanded to produce large areas without excessive structural defects. In order to accomplish these goals, the following studies are recommended:

1. Preparation or procurement of relatively defect-free ZnSe and/or AlAs crystals to provide large area junctions.

2. Parametric studies to determine optimum source and substrate temperatures for epitaxial depositions without damage to substrate properties.

3. Develop improved methods for preparing large-area, single-crystal thin films.

4. Construction of multielement device to demonstrate the writing, storage, reading, and erasing functions of devices utilizing electroluminescent junctions.

REFERENCES

(1) R. W. Haas and J. M. Hanlet, "Research on Low Voltage Electroluminescent Devices with Storage", NASA-CR-86060 (Contract No. NAS 12-545).

(2) J. M. Hanlet, "Research on Low Voltage Electroluminescent Devices with Storage" Final Technical Report - Phase II, NASA-CR-86344 (Contract No. NAS 12-545).

(3) R. F. Chicotka, "Crystal Growth and Characterization of AlAs" 137th meeting of the Electrochemical Society, Los Angeles, May 10-15, 1970.

(4) M. Ettenberg and S. Gilbert "Vapor-Phase Transport of High-Purity AlAs" 137th meeting of the Electrochemical Society, Los Angeles, May 10-15, 1970.

(5) H. C. Casey, Jr., and M. B. Panish, "Composition Dependence of the $Ga_{1-x}Al_xAs$ Direct and Indirect Energy Gaps", J. Appl. Phys. 10 , 4910, 1969.

(6) M. Hock and K. S. Hinge "Vaporization of AlAs" J. Chem Phys. 35, 45, 1961.

(7) A. G. Fischer, "Preparation and Properties of ZnS-Type Crystals from Melt" J. Electrochem. Soc. 106, 838, 1959.

(8) M. Hansen and K. Anderko, Constitution of Binary Alloys, 2nd Ed., McGraw-Hill Book Company, New York, 1958.

(9) R. P. Elliott, Constitution of Binary Alloys, First Supplement, McGraw-Hill Book Company, New York, 1965.

(10) H. P. Singh and B. Dayal, "X-Ray Determination of the Thermal Expansion of Zinc Selenide", Phys. Stat.Sol., 23 , K93 (1967).

(11) P. Goldfinger and M. Jennehomme, Trans. Faraday Soc. 59 2851 (1963).

(12) Handbook of Chemistry and Physics, 40th Edition, Chemical Rubber Publishing Co. 1958.

(13) D. Richman, "Vapor Phase Growth and Properties of Aluminum Phosphide", J. Electrochem. Soc. 115 , 945 (1968).

APPENDIX I

VAPORIZATION OF AlAs

VAPORIZATION OF AlAs

Thermodynamic calculations were made from the third law to estimate the equilibrium and partial pressure of the elements over AlAs, from the dissociation of AlAs according to:

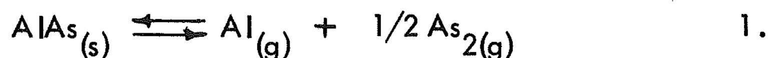

$$AlAs_{(s)} \rightleftharpoons Al_{(g)} + 1/2\, As_{2(g)} \qquad 1.$$

the dissociation constant is then given in atmosphere as a function of the activity, a, by,

$$K_d = \frac{a_{Al}\, a^{\frac{1}{2}}_{As_2}}{a_{AlAs}} = P_{Al} P^{\frac{1}{2}}_{As_2} \qquad 2.$$

Taking the activity of the pure solid compound as unity, the variation in free energy ΔG^o satisfying equation (1) is from Gibb's Law,

$$\Delta G^o = \Delta H^o \;\; -T \Delta S = -kT \;\ln (K_d) \qquad 3.$$

hence:

$$\ln(K_d) = \frac{-\Delta H^o}{kT} + \frac{\Delta S^o}{k} \qquad 4.$$

with ΔH^o & ΔS^o respectively the enthalpy and entropy change for Equation 1,

$$\log (K_d) = \log (P_{Al}\, P^{\frac{1}{2}}_{As_2}) = \frac{1}{2.3K} \left[- \frac{\Delta H^o}{T} + \Delta S^o \right] \qquad 5.$$

The minimum total pressure occurs over AlAs evaporating congruently, i.e., with a ratio of partial pressure of Al to As_2 of 2 to 1. Hence the minimum total pressure is,

$$(P_m)_T = P_{Al} + P_{As_2} = \frac{3}{2} P_{Al} = 3P_{As_2} \qquad 6.$$

Combining (6) with (2) with experimental data for K_d allows calculation of $(Pm)_T$.

The experimental data was obtained as a function of the evaporation rate from a Knudsen source, using a quartz microbalance, corroborated with interferometric measurements of film thickness.

The arsenic vapor within the range of temperature used, contains a negligible amount of monomeric arsenic, i.e., 1 part in 10^7. The tetramer contribution can be minimized by compacting the evaporant at 8,000 to 10,000 psi.

The pressure developed by effusion from a Knudsen chamber is:

$$p = m(2\pi RTM^{-1})^{\frac{1}{2}} \qquad 7.$$

This is related to the equilibrium pressure p_o by

$$p = p_o \left[\alpha (A_K/A)^{-1} + \alpha \right] \qquad 8.$$

Hence if:

$$Ak/A << \alpha \; p = p_o \qquad 9.$$

and if,

$$\alpha << A_K/A \qquad p = p_o \left[\alpha (A_K/A)^{-1} \right]$$

with the symbols:

m = mass evaporated in g cm^{-2} sec^{-1}
R = gas constant
T = temperature in ^oK
M = atomic mass
α = accommodation coefficient
A_K = area of the Knudsen aperture
A = area of evaporation

Within the range of temperature experimented with, by changing the ratio between the two areas, A_K/A, the relation

$$K_p = p_{Al} p^{\frac{1}{2}}_{As_2}$$

shows K and p to be independent of A_K/A, thus, a is found to be equal to or very close to unity. From the measured slope of the equilibrium constant plotted against 1/T, and Clausius-Clapeyron relation, a heat of reaction ΔH_{298} of 137.2 ± 1.5 Kcal was obtained for AlAs. The results of this analysis are shown in Figure 7 and are in good agreement with the experimental work of Hoch and Hinge.[6]

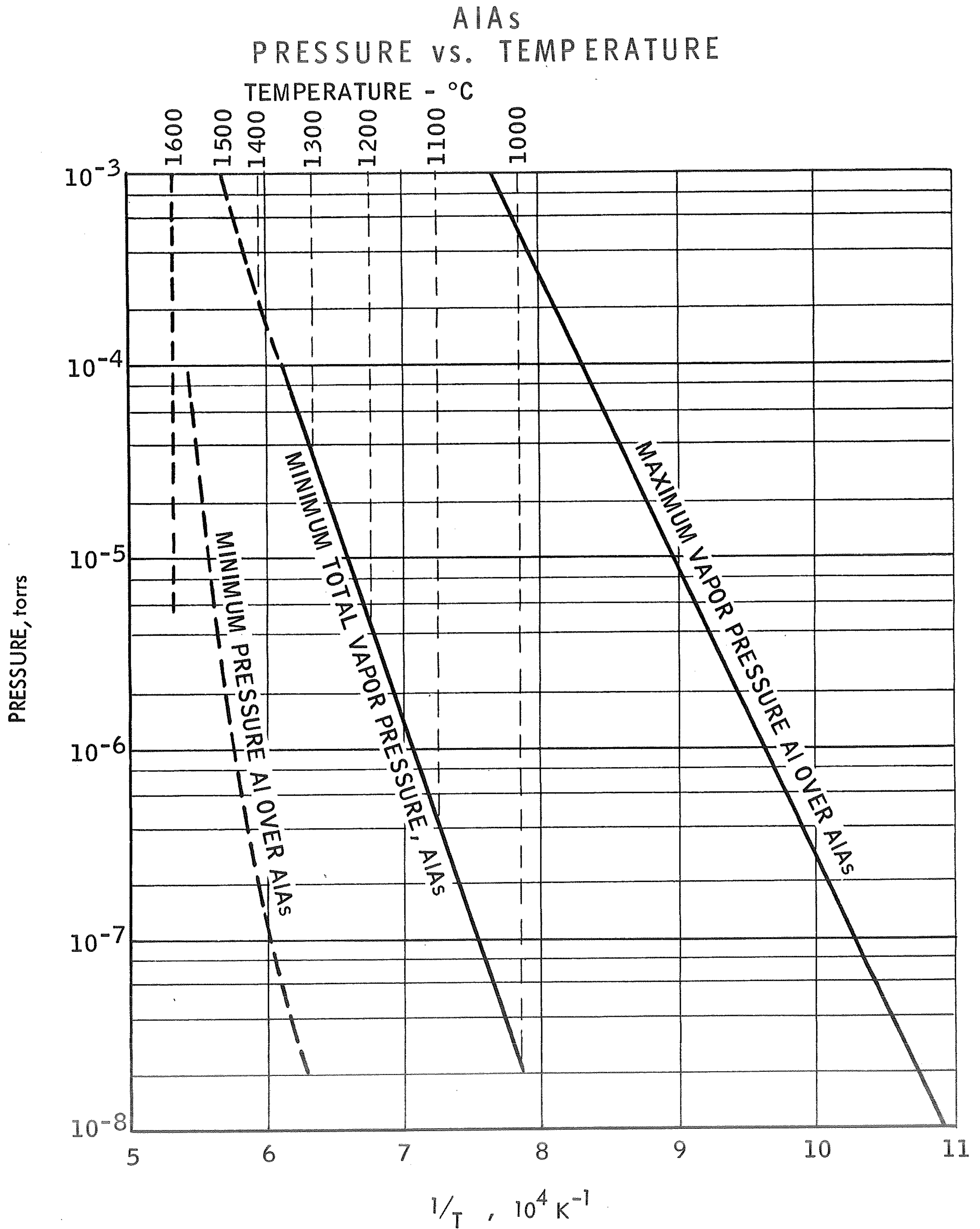

Figure 7

APPENDIX II

OPTICAL METHOD FOR DETERMINING BAND GAP

OPTICAL METHOD FOR DETERMINING BAND GAP

A method was developed for the determination of optical constants in complex films by measuring the transmittance from interference patterns. This method circumvents the need for the preparation of special specimens needed in magneto-resistance measurements. The method relies on the measurement of interference patterns in the combinations: air-film, film-substrate, and substrate-air. Assigning the subscripts 1, 2, 3 for air, film, and substrate, respectively, the thickness of the film, d, is obtained by condition of interference minimum from the relationship,

$$(2m + 1)\frac{\lambda}{4} = n_2 d \qquad 1.$$

where m is the order of interference, n, the index of refraction and λ the wave length. The minimum transmittance Tm is given by:

$$Tm = \frac{4n_2^2 \; n_3}{(n_2^2 + n_3)^2} \qquad 2.$$

The energy dependence of the absorption coefficient α assumed the form

$$\alpha = \alpha_o (\phi - \Delta E)^x \qquad 3.$$

With: ϕ the energy of the incident photons; ΔE the band gap energy; x is assigned a value of 1/2 or 3/2 for allowed or forbidden transition in a direct band to band transition.

The energy transmittance is

$$T = (1 - R_1)(1 - R_2)(1 - R_3)\left(1 + \frac{\alpha \lambda}{4\pi n_2^{\,2}}\right) \exp^{-\alpha d} \qquad 4$$

With R the reflection coefficient pertaining to the interfaces 1, 2, 3, obtained from the classical dispersion theory

$$R = \left[(n - 1)^2 + k^2\right] / \left[(n + 1)^2 + k^2\right] \qquad 5$$

With the dispersion index k

$$k = \frac{2\, T_R \sin \delta}{1 + T_R^{\,2} - 2\, T_R \cos \delta)} \qquad 6$$

where the phase difference δ is given by

$$\delta = 2\pi n d\, \lambda^{-1} \qquad 7$$

and T_R, the transmission ratio between minima and maxima is

$$T_R = \frac{T_m}{T_M} \qquad 8$$

Operating with films of different thickness in (4) gives the ratio of transmissions

$$\Delta T = (1 - R)^2 \exp^{-\alpha \Delta d} \simeq \exp^{-\alpha \Delta d} \qquad 9$$

from (3) we then have

$$\alpha \Delta d = \alpha_o \Delta d\, (\phi - \Delta E)^x \qquad 10$$

Plotting $(\alpha \Delta d)^{1/x}$ versus ϕ gives a straight line from which parameters α_o and ΔE can be obtained.

From the range of ϕ used in the measurement which extends from the absorption edge to the near infrared with the Beckmann DK1 we have

$$\mathcal{E} = n_2^{\,2} - k^2 = \mathcal{E}_o - \frac{4\pi N e^2}{m^* W^2} \qquad 11$$

where $\mathcal{E}_o$ is the optical dielectric constant; m* the carrier's effective mass; N the carrier's concentration; W is comprised between the collision frequency W_o and W_i the red limit of the fundamental absorption band

$$W_o < W < W_i \qquad 12$$

From (11) and (12) it follows that using (2) and (6) near the short wavelength of the infrared absorption band permits the plot $\mathcal{E}$ versus λ whose slope will allow the calculation of the effective mass m* for a known carrier concentration N. The collision frequency W_o can also be found from the known value of the mobility from

$$W_o = \frac{e}{m^* v} = \frac{e}{m^* \mu E} \qquad 13$$

with the velocity $v = \mu E$, with E the field applied.

This approach permits an appreciable time saving in calculating the film properties, since for $T < 0.1$ in (4) the error in calculating α is less than 0.001.

APPENDIX III

ELECTROLUMINESCENCE MODEL

ELECTROLUMINESCENT MODEL

As part of the objectives of this work, a demonstration electroluminescent device was constructed using a large area thin film of Ga-doped ZnSe deposited epitaxially on a single crystal sapphire plate cut on a basal plane. A pattern of platinum was deposited on the ZnSe film. The conditions of the deposition was such that a thin oxide layer could be expected thus resulting in a p-i-n junction. The other electrode material, indium, has a low work function resulting in an ohmic contact with the semiconductor. Of the sections formed, seven most active were used. A photograph of this model is shown in Figure 8. This activity was conducted at the end of the Phase II activities and reported as part of that effort. The p-i-n junction characteristics measured on this material is repeated here.

The height of the potential barrier, Φ, through which the charge carriers gain their kinetic energy is expressed by

$$eV_D \geqslant \Phi = \phi_m - \phi_s \qquad 1$$

with: V_D the diffusion potential; e the elementary charge; ϕ_m the metal work function; ϕ_s the semiconductor work function, $\phi_s \simeq X + E_F$, where $X = \Phi - E \asymp \phi_s - E_F$ with X, E and E_F respectively the semiconductor electron affinity, its band gap and Fermi level.

The surface state influences profoundly the work functions of both metal and semiconductor, as a result, the potential barrier is seldom calculable from the work function above.

The characteristics of such junctions are accessible through barrier capacitance measurements, from derivation of Poisson's equation:

$$\frac{d^2\Psi}{dx^2} = \frac{eNd}{\epsilon\,\epsilon_o} \qquad 2$$

with: $\Psi = (V_D + V)$ at $x = d$; d the barrier thickness; V the applied voltage; Nd the donor density; ϵ the dielectric constant of ZnSe; ϵ_o free space permitivity we have

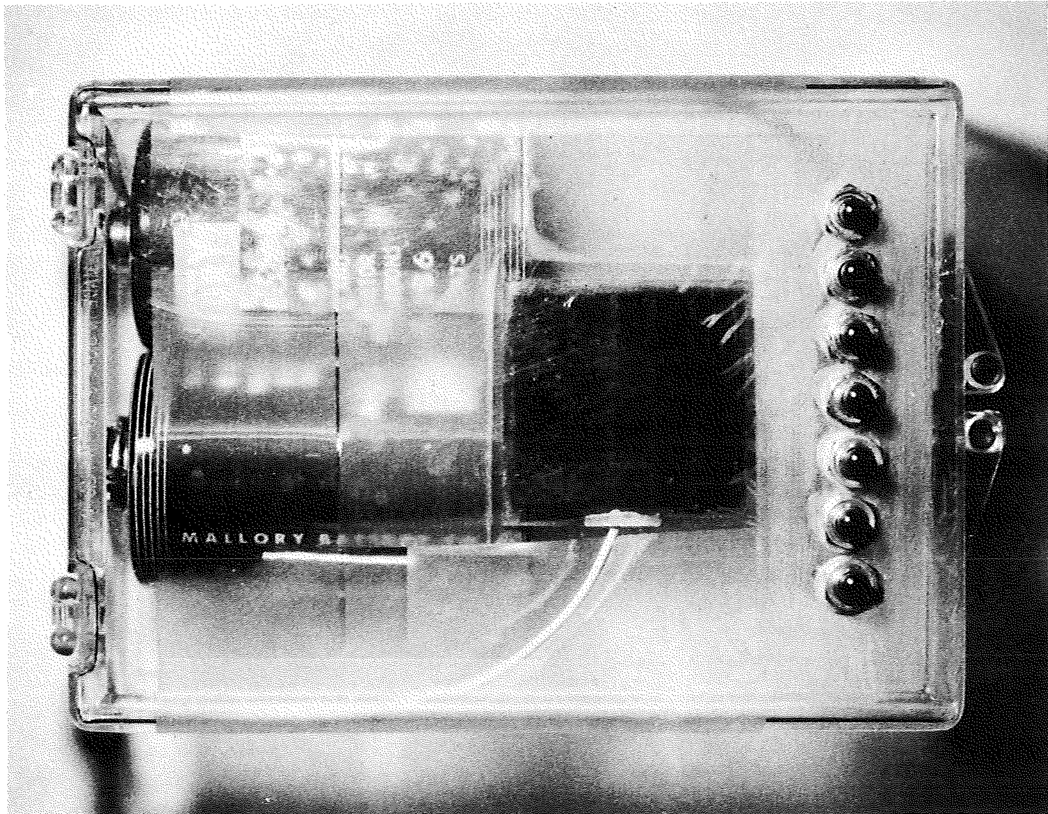

Figure 22

ELECTROLUMINESCENT MODEL

$$(V_D + V) = \frac{eN_d}{2\epsilon\epsilon_o} d^2 \qquad 3$$

Since the charge Q per unit area is

$$Q = eN_d\, d = \left[2\epsilon\,\epsilon_o\, eN_d (V_D + V)\right]^{1/2} \qquad 4$$

the junction capacitance follows from

$$C = \frac{dQ}{dV} = \left[\frac{e\,\epsilon\,\epsilon_o\, N_d}{2\,(V_D + V)}\right]^{1/2} \qquad 5$$

the thickness of the barrier is obtained from equation (3) as

$$d = \left[\frac{2\,\epsilon\,\epsilon_o}{eN_d}\,(V_D + V)\right]^{1/2} \qquad 6$$

Equation (5) may be written in the form,

$$\frac{d\,(1/C^2)}{dV} = \frac{2}{e\,\epsilon\,\epsilon_o\, N_d} \qquad 7$$

from which the carrier concentration gives

$$N_d = \frac{2}{e\epsilon\,\epsilon_o}\,\frac{dV}{d\,(1/C^2)} \qquad 8$$

extrapolating $1/C^2$ to zero gives the value of the diffusion potential V_D.

The current voltage relationship in such electroluminescent diodes is represented by

$$I = I_o \left(\exp^{-\frac{eV}{kT}} - 1\right) \qquad 9$$

where the saturation current I_o is obtained from the equation

$$I_o = \left(\frac{4\pi e\, m^*\, k^2}{h^3}\right) T^2 \exp^{-\frac{\phi_m - X}{kT}} \qquad 10$$

with m* the effective mass; k Boltzmann's constant; h Planck's constant; T the temperature.

The probability of generating electroluminescence by field ionization when operating the diode in the reverse direction may be calculated from

$$p = \frac{eEdn}{h} \exp\left[-\frac{\pi^2}{2ehE} \sqrt{2m^*}\; Eg^{3/2}\right] \qquad 11$$

with E the field strength $E = (2V_D + V)/d$ across the junction; dn the nearest neighbor distance $dn = a_o \sqrt{3}/4$ with a_o the lattice constant of ZnSe $a_o \approx 5.658\,\mathring{A}$.

Measurements were performed with a Boonton bridge at 1 Mc sec^{-1} with a built-in DC power supply providing the voltage V. The capacitance of a junction area approximately 5×10^{-3} cm^2 has been plotted as a function of voltage, Figure 9(a), introducing the constants $\epsilon = 8.7$ for ZnSe; $\epsilon_o \approx 8.85 \times 10^{-14}$ Fd cm^{-2} in the function $1/C^2 = f(V)$ yields a carrier concentration $Nd \approx 10^{18}$ cm^{-3} with about one order of magnitude discrepancy from resistivity measurements. From extrapolation of $1/C^2$, Figure 9(b), a diffusion voltage of 1.98 volts is found, whereas extrapolating the function current voltage (Figure 10) a value of 2.1 volts is obtained; the discrepancy between the two values is small and well within the errors due to the small

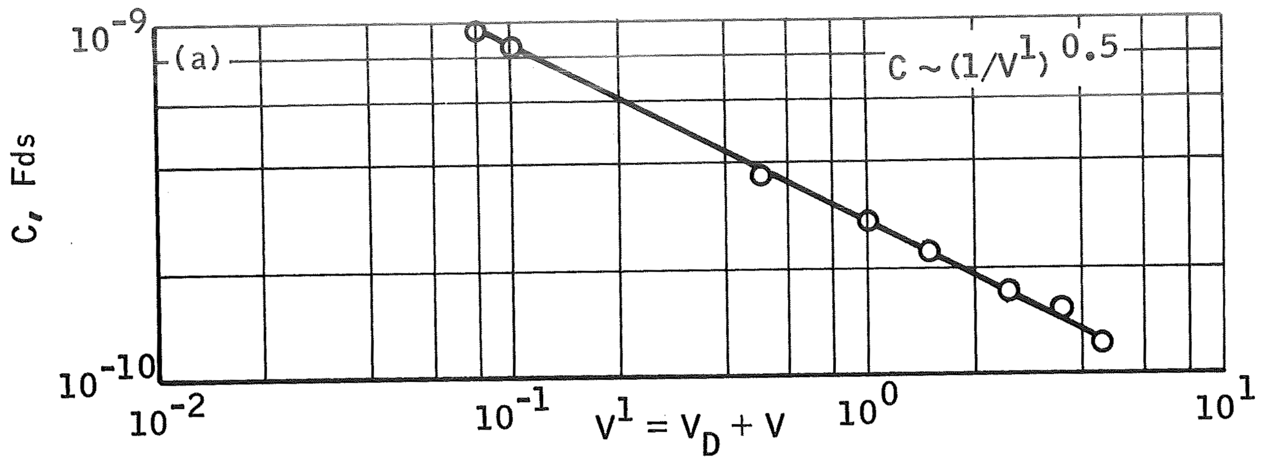

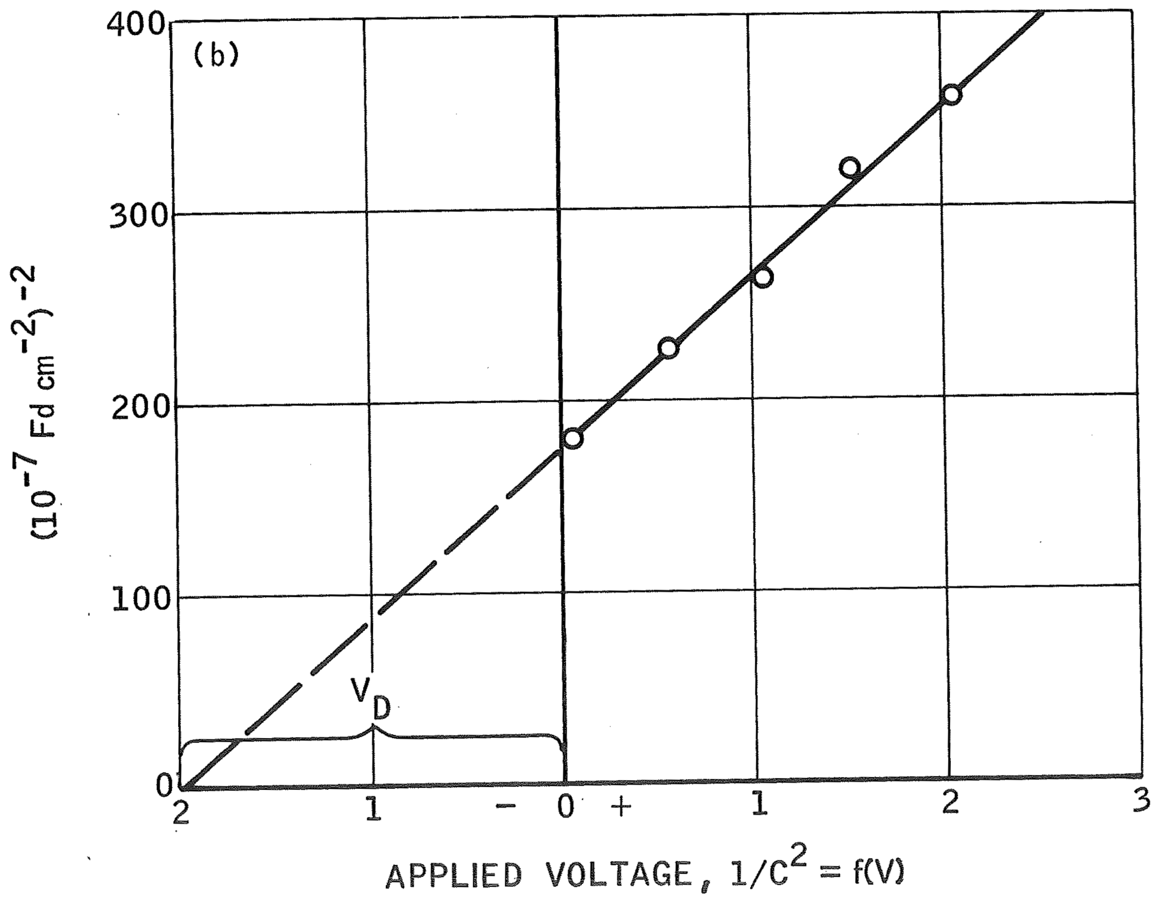

CAPACITANCE vs. VOLTAGE ACROSS JUNCTION

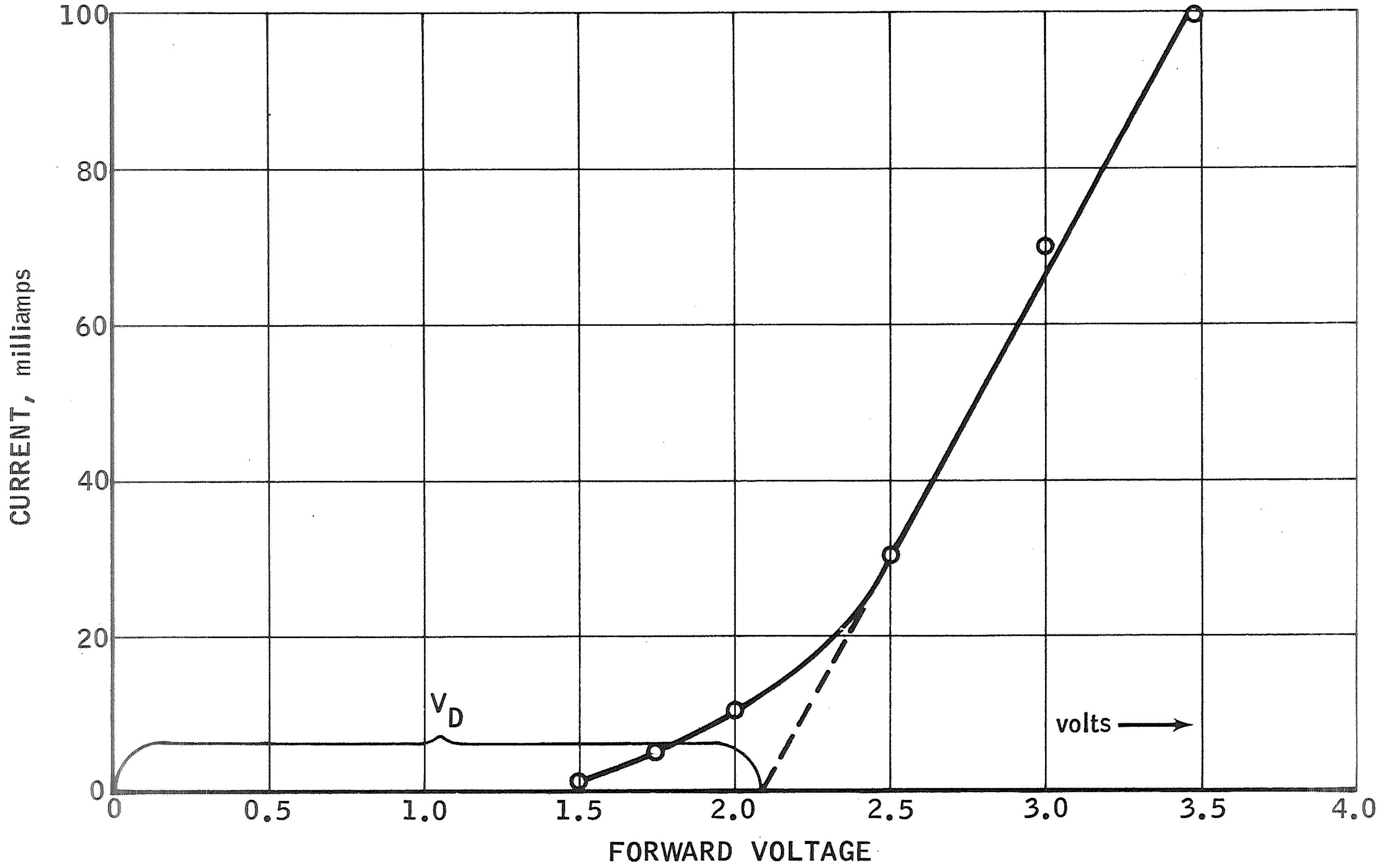

pin DIODE VOLTAGE-CURRENT RELATIONSHIP

Figure 10

THE Marquardt CORPORATION
VAN NUYS, CALIFORNIA

junction area. With a barrier's thickness calculated from equation (6) of $\approx 4 \times 10^{-4}$ cm the probability from equation (11) approaches unity as the voltage approaches 20 volts.

The current voltage relationship for the diodes tested is shown in Figure 10 and emission spectrum plotted at room temperature in Figure 11.

The brightness has been measured by bringing in the vicinity of the diode surface a fiber optics coupled with the photomultiplier of a Gamma photometer. The brightness has been plotted as a funtion of the diode current in Figure 12. This plot indicated a light intensity proportional to the current within the range of current investigated.

The efficiency of the electroluminescent diode was evaluated, taking into account the spectral response and the steradiancy between junction's plane and fiber optics from

$$k = \frac{BSQ\ 10^{17}}{1.26L} \qquad 12$$

where k represents the number of quanta emitted per second; Q the integrated quantum output in $d\lambda$; L the luminosity factor of the spectrum; B the brightness in foot Lambert.

The measurements were repeated within the linear range shown in Figure 12 to give

$$\frac{ek}{i} \times 100 = \text{efficiency in percent} \qquad 13$$

with i the current in amperes.

The efficiency of the diodes tested was found to vary between 0.1 to 0.05 percent, i.e., 10^4 or more electrons per photon.

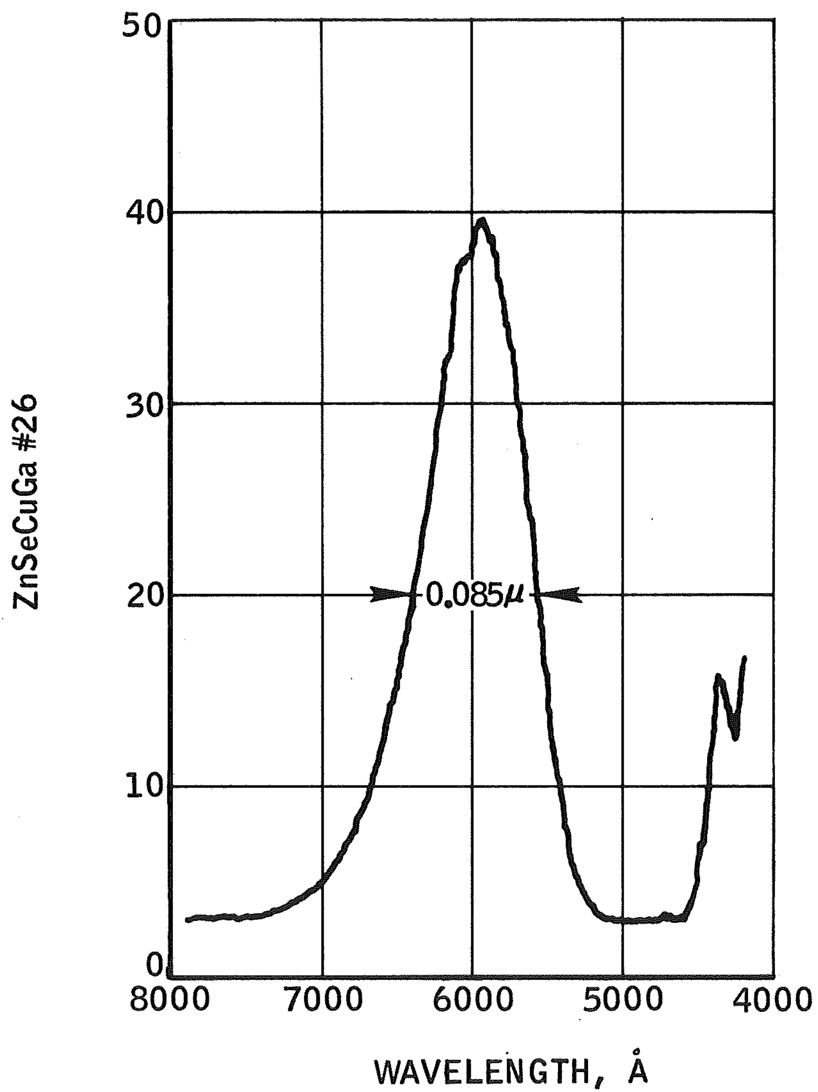

pin DIODE ZnSeGa SPECTRAL EMISSION

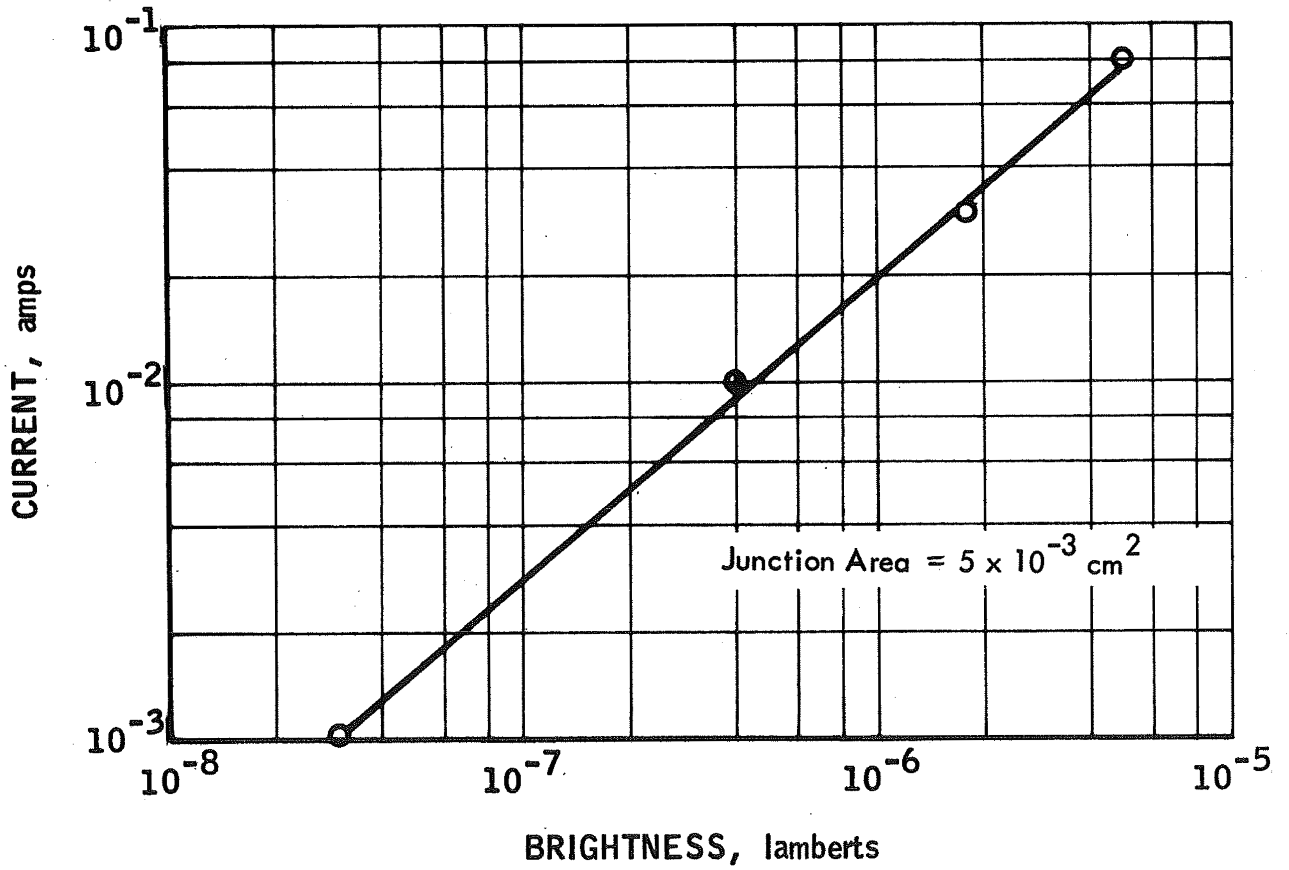

CURRENT-BRIGHTNESS RELATIONSHIP

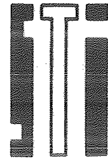

APPENDIX IV

NEW TECHNOLOGY

After a diligent review of the work performed under this contract, no new innovation, discovery, improvement or invention was made.